Binding affinity assay of SARS-CoV-2 spike protein and amyloid-β using affinity capillary electrophoresis – vibrating sharp-edge spray ionization – mass spectrometry (ACE-VSSI-MS)

Makenzie T. Witzel

ABSTRACT. This research proposes a method to quantify the dissociation constant (K_d) between SARS-CoV-2 spike protein (S protein) and amyloid-$\beta_{(1-42)}$ ($A\beta_{42}$) using affinity capillary electrophoresis – vibrating sharp-edge spray ionization – mass spectrometry (ACE-VSSI-MS). Mobility shift ACE enables the rapid and simple on-line determination of K_d with little sample consumption. This proposed research has 2 aims: (1) Develop a method to perform mobility shift ACE using VSSI-MS detection to couple the high throughput benefits of CE and structural insight MS detection provides and (2) quantify the dissociation constant of S protein and $A\beta_{42}$ to inform on binding affinity and further research in understanding long COVID symptoms.

1 | INTRODUCTION

SARS-CoV-2, the novel coronavirus of the COVID-19 pandemic, initiates viral infection through binding between the spike protein receptor binding domains (RBDs) and angiotensin-converting enzyme 2 (ACE2), a cell membrane protein found throughout the body.[1,2] Spike protein (S protein) also binds proteins and peptides that are not ACE2, like amyloid-$\beta_{(1-42)}$ ($A\beta_{42}$)[3], which can intensify the effects and prolong the after-effects of viral infection.[3–5] The SARS-CoV-2 pandemic has resulted in millions of cases and over 400 thousand instances of symptoms persisting for months after initial infection which has been termed post COVID-19 condition or "long COVID" as of August 2024.[6] One long COVID symptom is brain fog, which has been found to be caused by abnormal electroencephalographic activity and resembles abnormalities seen during early stages of neurodegenerative diseases.[7,8] During viral invasion, S protein can be cleaved by proteases into several amyloidogenic peptides that are linked to increased $A\beta_{42}$ fibril and plaque formation, contributing to neurodegeneration.[2,4,5,9–12]

Little has been published on the binding interaction between SARS-CoV-2 S protein and $A\beta_{42}$, and these publications are focused on either the increased virility of the SARS-CoV-2 virus due to $A\beta_{42}$ binding[3,8,13] or the amyloidogenic peptide fragments of digested S protein accelerating $A\beta_{42}$ fibrilization and neurodegeneration associated with Alzheimer's Disease (AD) as described above. These publications, however, do not explore the binding kinetics of S protein and $A\beta_{42}$. One publication quantified the diffusion constant of S protein and $A\beta_{42}$ fibrils through molecular dynamics simulations and focused on the orientation of binding.[2] While the diffusion constant influences binding, it is not a direct measure of the binding affinity.

Studies have been published regarding S protein binding affinity with other molecules such as α-synuclein, which could be viewed as the equivalent to $A\beta_{42}$ in Parkinson's Disease[14], and heparin, a glycosaminoglycan that interacts with $A\beta_{42}$ to increase aggregation.[15] The dissociation constants of α-synuclein and S protein RBD determined by isothermal titration calorimetry was 503±24 nM[16] and heparin determined by surface plasmon resonance ranged 40 pM[17] to 64 nM.[18] While these are examples of dissociation constants of S protein or the S protein RBD and a ligand, $A\beta_{42}$ is not necessarily going to behave similarly considering its smaller mass and less negative charge. Additionally, it has been demonstrated that K_d determined with the RBD does not predict the K_d of the whole S protein.[17–19] A quantified dissociation constant would provide insight into the interaction and affinity between S protein and $A\beta_{42}$ and inform future research regarding SARS-CoV-2 virility, $A\beta_{42}$ suppressant drug therapies,[16,20,21] and contribution of long COVID in neurodegeneration.

There are many techniques used for affinity measurements including equilibrium dialysis,[22–24] ultrafiltration,[22–24] calorimetry,[24] size and affinity chromatography,[22,24] slab gel electrophoresis,[25,26] and spectroscopic methods such as UV-Vis and infrared absorbance, fluorescence, circular dichroism, nuclear magnetic resonance, and surface plasmon resonance.[23,24] Most of these technologies are inconvenient due to slow analysis time,[24] requirements of large amounts of sample,[24] incapability to analyze multiple sample components,[27] or are expensive to execute.[24]

An alternative approach is affinity capillary electrophoresis (ACE), a well-developed method for quantifying protein and peptide interactions;[22–26,28–32] however, it has been sparsely applied to S protein and its possible ligands. Benefits of ACE include no requirement of ligand immobilization to a stationary phase to prevent affecting binding properties,[23,27] low volume sample consumption, simulation of physiological conditions,[23,27,33] on-line detection,[33] and applicability to a wide variety of analytes.[22] ACE can be broken down into dynamic equilibrium, pre-equilibrated, and kinetic techniques.[22–24,32] In pre-equilibrated ACE methods, the receptor and ligand are equilibrated off-line and CE is used to separate the free and bound analytes. These techniques are best suited for analytes with slow equilibrium kinetics and strong affinity to have enough time to associate and not dissociate during the separation with the most common applications being frontal analysis ACE and affinity probe capillary electrophoresis. Dynamic equilibrium ACE includes a ligand in the background electrolyte and relies on mobility shift to determine the dissociation constant. The receptor exists in a free or bound state and the duration of time spent in each state will change with changing ligand concentration. This method is best for fast kinetics and weak to intermediate binding affinity. Dynamic techniques include mobility shift ACE, vacancy peak methods, and the Hummel-Dreyer method. Kinetic techniques are used for intermediate reaction rates where the time to reach binding equilibrium is similar to the migration time.[23] Methods include nonequilibrium and equilibrium CE of

equilibrium mixtures (NECEEM), partial-filling ACE, and multi-step ligand injection ACE (MSLIACE). Of these methods, mobility shift ACE is what will be implemented in this study since the binding affinity of these molecules is unknown and the method is simple in design, easily adaptable, and produces results quickly. This method is well suited for these analytes considering that bound $A\beta_{42}$ will increase the mass and negative charge of S protein as well as induce a conformation change upon binding **(Figure 1)**[34] which contribute to the mobility shift.

Nanoflow sheath capillary electrophoresis – vibrating sharp-edge spray ionization – mass spectrometry (CE-VSSI-MS) is an established technique for small molecule[35] and protein[36] separations using both unmodified and coated capillaries. VSSI is a voltage-free, soft, ambient ionization method where acoustic energy is focused at a sharp edge to produce a spray.[37,38] Ionization is independent of solvent composition, making this technique applicable to native analysis and avoids analyte denaturation attributed to the applied voltages of ESI.[39] Additionally, it had been demonstrated that VSSI can keep non-covalently associated complexes intact from the solution phase to the gas phase,[39] similar to electrospray ionization,[23,32,40] which is beneficial when detecting bound complexes with ACE. Native mass spectrometry detection adds the benefits of assigning accurate molecular weight and elucidating native structure,[23,27,41,42] identification of multiple or heterogeneous analytes,[23,27,32,41] and requiring no sample derivatization such as fluorescent labeling for analyte visualization.[24,41]

This work proposes the first use of nanoflow CE-VSSI-MS for fast and simple affinity binding by mobility shift ACE, broadening the capabilities of this instrumentation. This will be the first dissociation constant quantification of the novel SARS-CoV-2 S protein and $A\beta_{42}$.

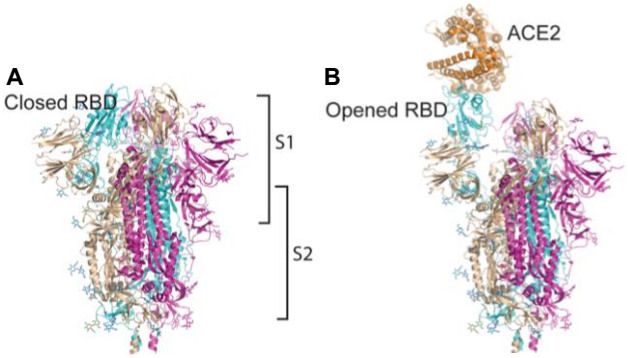

FIGURE 1 (A) Closed S protein conformation vs (B) open S protein conformation with bound ligand. Adapted from Huang et al.[34]

2 | PROPOSED RESEARCH

2.1 | Aim 1: Development of a separation method to quantify binding between S protein and $A\beta_{42}$

2.1.1 | Significance

Coupling of ACE and MS for protein – peptide binding interactions is not a commonly used technique in the literature. This will be the first use of VSSI-MS for affinity CE of SARS-CoV-2 S protein and $A\beta_{42}$.

2.1.2 | Experimental approach

Traditional CE instrumentation adapted for MS detection will be used (**Figure 2**). Briefly, the outlet of the separation capillary is not in a background electrolyte vial. This allows for the VSSI source to spray the solution at the outlet of the capillary. The nanoflow sheath supplies a makeup flow to increase the flow rate to sustain stable ionization.[35] A bare-fused silica capillary will be used, and the electroosmotic flow will not be suppressed at physiological pH. The analytes should not exhibit surface adsorption to the uncoated capillary since they are negative or neutral. Considering this, a normal polarity separation voltage will be applied for the electroosmotic flow to be directed toward the detector. Under these conditions, cationic analytes will be detected first, then neutral, then anionic.

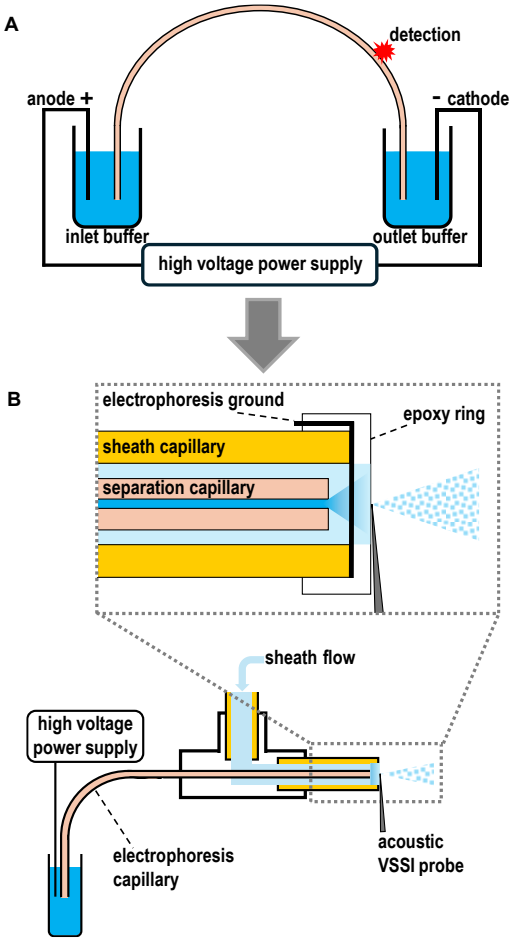

FIGURE 2 **(A)** Commercial CE instrumentation adapted for **(B)** mass detection. The analyte is ionized and transferred from the capillary to the mass spectrometer by VSSI. Figure adapted from Witzel et al.[36]

The ACE separation is designed so that S protein (the receptor) will interact with $A\beta_{42}$ (the ligand) as it travels through the capillary. $A\beta_{42}$ is included in the background electrolyte at varying concentrations, and a plug of S protein is injected by pressure and electrophoresed through the capillary **(Figure 3A)**. As S protein migrates, it will interact with the $A\beta_{42}$ in solution, which affects the protein mobility. $A\beta_{42}$ is negatively charged at physiological pH, therefore, the shift in mobility will be

facilitated by the increased negative charge and increase in hydrodynamic radius[29,43] during interaction, both contributing to slowing down the migration of S protein. S protein will also change to open conformation when bound[34] which will further increase the hydrodynamic radius and contribute to the slower migration time. The degree of the change in migration will correlate with the binding between S protein and $A\beta_{42}$, where more binding, presumably at higher concentrations, will cause the S protein to slow down and be detected at a later migration time **(Figure 3B)**.

An internal standard, mesityl oxide, is included in the separation to account for possible variation in electroosmotic flow at different $A\beta_{42}$ concentrations.[29,43] This internal standard does not interact with the ligand and in this case will be neutral, so it will not have an electrophoretic mobility.

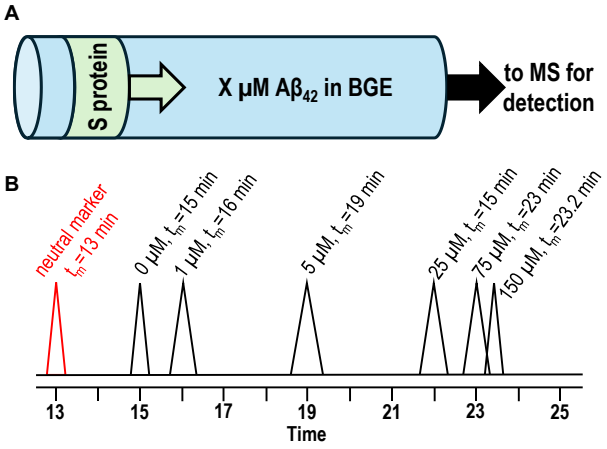

FIGURE 3 **(A)** Capillary patterning for ACE binding assay. **(B)** Hypothetical data set demonstrating the effect of increasing Ab concentration on S protein mobility. Peak broadening may be seen due to slow dissociation kinetics where a similar population of both free and bound receptors are present at detection. A solution to peak broadening is to increase the separation time to allow more time for equilibration.[22,23,32,43]

The electrophoretic mobility (μ_{eph}) of S protein at each $A\beta_{42}$ concentration is calculated using **Eq. (1)**.

$$\mu_{\text{eph}} = \frac{L_t L_d}{V}\left(\frac{1}{t_p} - \frac{1}{t_{eof}}\right) \left[\text{cm}^2\text{V}^{-1}\text{s}^{-1}\right] \quad \textbf{(1)}$$

L_t is the total capillary length, L_d is the length to the detector, V is the applied voltage, t_p is the migration time of S protein, and t_{eof} is the migration time of the neutral marker. The mobility of the neutral marker is subtracted from the mobility of S protein. This removes the contribution of electroosmotic flow to the mobility of S protein so that only electrophoretic mobility is considered when plotting the binding constant curve.

Dynamic ACE coupled to MS can present a few challenges. One being the persistent detection of ligand since it is charged and will migrate. $A\beta_{42}$ will be included in the background electrolyte at low concentration, and the m/z will be much lower than what will be detected for S protein so it can be isolated. Competitive ionization could also cause concern; however, mobility shift ACE is not dependent on peak area quantitation to determine the dissociation constant.[22,32] Therefore, if the analyte peak can be detected, this method is valid. Another challenge can be the interaction of the analyte with the unmodified silica surface of the capillary. While the anionic analytes used in this study should not suffer from surface adsorption, it would be a concern if this method were applied to positively charged analytes. This can be solved by capillary coatings to neutralize the surface charge. This also suppresses the electroosmotic flow, so a neutral marker can no longer be used to correct for electroosmotic flow in the calculation of electrophoretic mobility shift. Instead, a similarly charged molecule to the analyte that does not exhibit interaction with the ligand can be used, or the electroosmotic flow, if any is present, can be calculated separately from the separation using a 3 peak method developed by Williams et al.[44]

2.2 | Aim 2: K_d determination

2.2.1 | Significance

This work proposes the first K_d quantitation of SARS-CoV-2 S protein and $A\beta_{42}$. There is currently no published dissociation constant for these molecules and revealing this data can assist in better understanding the physiological relevance and implications of this interaction, possibly assisting research in neurodegeneration associated with long COVID or worsening of SARS-CoV-2 infection due to changes in viral binding.

2.2.2 | Experimental approach

Determining the dissociation constant is imperative because it quantifies the strength of binding, providing insight into the biological function of a molecular interaction. Quantifying the K_d for SARS-CoV-2 S protein and $A\beta_{42}$ can help to understand the effects this interaction has on exacerbated viral infection and prolonged after-effects.

It seems there is no reported dissociation constant for SARS-CoV-2 whole S protein and $A\beta_{42}$. To establish a starting point for this study, K_d constants from literature for molecules involved in similar biological pathways will be referenced despite spanning a wide range. Heparin is reported to have a K_d of 40 pM[17] to 64 nM[18] while α-synuclein has a K_d of 503±24 nM.[16] $A\beta_{42}$ is much smaller than both references at 4514 Da compared to 14000 to 16000 Da heparin and 14460 Da α-synuclein and is also less negatively charged at physiological pH. These properties will affect binding and the dissociation constant, and the concentration of both receptor and ligand will likely need adjustment based on the experimental data. The concentration of ligand should be included in the background electrolyte in excess relative to the receptor to prevent ligand depletion.

The binding constant will be determined by plotting the S protein mobility shift ($\Delta\mu_{eph}$) against the concentration of $A\beta_{42}$ in the background electrolyte. The mobility shift is calculated by subtracting the mobility of S protein with no ligand from the mobility of S protein at each ligand concentration. A K_d curve typically uses the fraction of binding sites occupied by the ligand as the y-axis variable. Analyte mobility shift can be translated to fraction bound by **Eq. (2)**[45],

$$\theta = \frac{\mu_{\text{eph}} - \mu_{\text{free}}}{\mu_{\text{max}} - \mu_{\text{free}}} \quad \textbf{(2)}$$

where θ is the fraction of bound analyte on a scale of 0 to 1, μ_{eph} is the observed electrophoretic mobility of the analyte, μ_{free} is the electrophoretic mobility of the analyte with no ligand interaction, and μ_{max} is the electrophoretic mobility of the analyte at maximum binding. For this study and the examples included in this proposal, mobility shift will be used as the y-axis variable, not fraction bound. Data points will be collected surrounding the hypothesized K_d value based on published data, with an emphasis on the data points on the slope of the fitted curve. This is because the slope of the curve is sensitive and the more data points there are to guide the fit, the more accurate the calculated K_d constant will be.

The data can be fitted using a non-linear regression model following **Eq. (3)**, assuming that the binding is specific and 1:1 to determine the experimental K_d from the fitted data points.

$$\Delta\mu_{\mathrm{eph}} = \frac{B_{\max} X}{K_d + X} \quad \textbf{(3)}$$

$\Delta\mu_{eph}$ is the difference in mobility between separation conditions of 0 μM $A\beta_{42}$ in the background electrolyte and including $A\beta_{42}$ in the background electrolyte at X concentration, B_{max} is the maximum mobility shift or maximum binding, and K_d is the dissociation constant. Nonlinear regression is the more accurate method to determine K_d when compared to linear regression,[23,46] minimizing error and bias in the K_d measurement. **Figure 4** includes a hypothetical data set demonstrating this. As mentioned previously, more data points will be included, specifically two concentrations of $A\beta_{42}$ above and below the K_d to ensure the curve is accurately plotted. Additionally, the curve will be produced in triplicate to demonstrate method reproducibility and an average K_d.

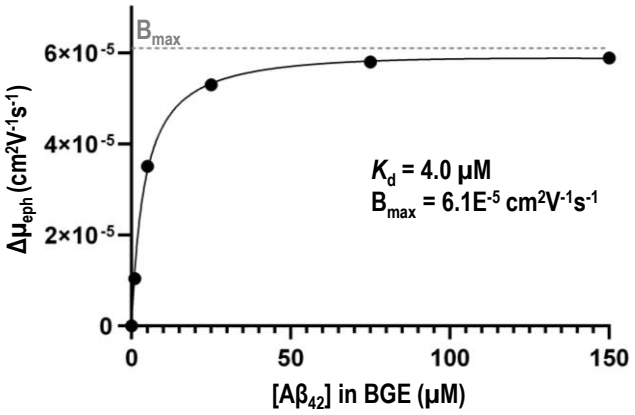

FIGURE 4 Hypothetical data set demonstrating a K_d curve and corresponding K_d and B_{max} values of 4.0 μM and 6.1E-5 $cm^2V^{-1}s^{-1}$ respectively. The data was fitted using GraphPad Prism 10.5.0.

References

(1) Shirbhate, E.; Pandey, J.; Patel, V. K.; Kamal, M.; Jawaid, T.; Gorain, B.; Kesharwani, P.; Rajak, H. Understanding the Role of ACE-2 Receptor in Pathogenesis of COVID-19 Disease: A Potential Approach for Therapeutic Intervention. *Pharmacological Reports* **2021**, *73* (6), 1539. https://doi.org/10.1007/S43440-021-00303-6.

(2) Coppola, F.; Pavlíček, T.; Král, P. Coupling of SARS-CoV-2 to Aβ Amyloid Fibrils. *ACS Omega* **2024**, *9* (8), 9295–9299. https://doi.org/10.1021/ACSOMEGA.3C08481.

(3) Hsu, J. T. A.; Tien, C. F.; Yu, G. Y.; Shen, S.; Lee, Y. H.; Hsu, P. C.; Wang, Y.; Chao, P. K.; Tsay, H. J.; Shie, F. S. The Effects of Aβ1-42 Binding to the SARS-CoV-2 Spike Protein S1 Subunit and Angiotensin-Converting Enzyme 2. *Int J Mol Sci* **2021**, *22* (15). https://doi.org/10.3390/IJMS22158226.

(4) Cao, S.; Song, Z.; Rong, J.; Andrikopoulos, N.; Liang, X.; Wang, Y.; Peng, G.; Ding, F.; Ke, P. C. Spike Protein Fragments Promote Alzheimer's Amyloidogenesis. *ACS Appl Mater Interfaces* **2023**, *15* (34), 40317–40329. https://doi.org/10.1021/ACSAMI.3C09815.

(5) Adewoye, A.; Ezeigbo, E.; Vo, Q. H.; Legleiter, J. Amyloidogenic SARS-CoV-2 Spike Protein-Derived Peptides Form Oligomers and Selectively Damage Lipid Membranes. *Biochemistry* **2025**, *64* (16), 3610–3622. https://doi.org/10.1021/ACS.BIOCHEM.5C00290.

(6) Al-Aly, Z.; Davis, H.; McCorkell, L.; Soares, L.; Wulf-Hanson, S.; Iwasaki, A.; Topol, E. J. Long COVID Science, Research and Policy. *Nat Med* **2024**, *30* (8), 2148–2164. https://doi.org/10.1038/S41591-024-03173-6.

(7) Jiang, Y.; Neal, J.; Sompol, P.; Yener, G.; Arakaki, X.; Norris, C. M.; Farina, F. R.; Ibanez, A.; Lopez, S.; Al-Ezzi, A.; Kavcic, V.; Güntekin, B.; Babiloni, C.; Hajós, M. Parallel Electrophysiological Abnormalities Due to COVID-19 Infection and to Alzheimer's Disease and Related Dementia. *Alzheimer's & Dementia* **2024**, *20* (10), 7296–7319. https://doi.org/10.1002/ALZ.14089.

(8) Idrees, D.; Kumar, V. SARS-CoV-2 Spike Protein Interactions with Amyloidogenic Proteins: Potential Clues to Neurodegeneration. *Biochem Biophys Res Commun* **2021**, *554*, 94–98. https://doi.org/10.1016/J.BBRC.2021.03.100.

(9) Larsson, J.; Hellstrand, E.; Hammarström, P.; Nyström, S. SARS-CoV-2 Spike Amyloid Fibrils Specifically and Selectively Accelerates Amyloid Fibril Formation of Human Prion Protein and the Amyloid β Peptide. *bioRxiv* **2023**, 2023.09.01.555834. https://doi.org/10.1101/2023.09.01.555834.

(10) Chiricosta, L.; Gugliandolo, A.; Mazzon, E. SARS-CoV-2 Exacerbates Beta-Amyloid Neurotoxicity, Inflammation and Oxidative Stress in Alzheimer's Disease Patients. *International Journal of Molecular Sciences 2021, Vol. 22, Page 13603* **2021**, *22* (24), 13603. https://doi.org/10.3390/IJMS222413603.

(11) Bhardwaj, T.; Gadhave, K.; Kapuganti, S. K.; Kumar, P.; Brotzakis, Z. F.; Saumya, K. U.; Nayak, N.; Kumar, A.; Joshi, R.; Mukherjee, B.; Bhardwaj, A.; Thakur, K. G.; Garg, N.; Vendruscolo, M.; Giri, R. Amyloidogenic Proteins in the SARS-CoV and SARS-CoV-2 Proteomes. *Nat Commun* **2023**, *14* (1), 1–16. https://doi.org/10.1038/S41467-023-36234-4;TECHMETA.

(12) Milton, N. G. N. SARS-CoV-2 Amyloid, Is COVID-19-Exacerbated Dementia an Amyloid Disorder in the Making? *Frontiers in Dementia* **2023**, *2*. https://doi.org/10.3389/FRDEM.2023.1233340/FULL.

(13) Clausen, T. M.; Sandoval, D. R.; Spliid, C. B.; Pihl, J.; Perrett, H. R.; Painter, C. D.; Narayanan, A.; Majowicz, S. A.; Kwong, E. M.; McVicar, R. N.; Thacker, B. E.; Glass, C. A.; Yang, Z.; Torres, J. L.; Golden, G. J.; Bartels, P. L.; Porell, R. N.; Garretson, A. F.; Laubach, L.; Feldman, J.; Yin, X.; Pu, Y.; Hauser, B. M.; Caradonna, T. M.; Kellman, B. P.; Martino, C.; Gordts, P. L. S. M.; Chanda, S. K.; Schmidt, A. G.; Godula, K.; Leibel, S. L.; Jose, J.; Corbett, K. D.; Ward, A. B.; Carlin, A. F.; Esko, J. D. SARS-CoV-2 Infection Depends on Cellular Heparan Sulfate and ACE2. *Cell* **2020**, *183* (4), 1043-1057.e15. https://doi.org/10.1016/j.cell.2020.09.033.

(14) Meade, R. M.; Fairlie, D. P.; Mason, J. M. Alpha-Synuclein Structure and Parkinson's Disease - Lessons and Emerging Principles. *Mol Neurodegener* **2019**, *14* (1). https://doi.org/10.1186/S13024-019-0329-1.

(15) Nguyen, K.; Rabenstein, D. L. Interaction of the Heparin-Binding Consensus Sequence of β-Amyloid Peptides with Heparin and Heparin-Derived Oligosaccharides. *J Phys Chem B* **2016**, *120* (9), 2187–2197. https://doi.org/10.1021/ACS.JPCB.5B12235.

(16) Mesias, V. S. D.; Zhu, H.; Tang, X.; Dai, X.; Liu, W.; Guo, Y.; Huang, J. Moderate Binding between Two SARS-CoV-2 Protein Segments and α-Synuclein Alters Its Toxic Oligomerization Propensity Differently. *J Phys Chem Lett* **2022**, *13* (45), 10642–10648. https://doi.org/10.1021/ACS.JPCLETT.2C02278.

(17) Kim, S. Y.; Jin, W.; Sood, A.; Montgomery, D. W.; Grant, O. C.; Fuster, M. M.; Fu, L.; Dordick, J. S.; Woods, R. J.; Zhang, F.; Linhardt, R. J. Characterization of Heparin and Severe Acute Respiratory Syndrome-Related Coronavirus 2 (SARS-CoV-2) Spike Glycoprotein Binding Interactions. *Antiviral Res* **2020**, *181*, 104873. https://doi.org/10.1016/J.ANTIVIRAL.2020.104873.

(18) Liu, L.; Chopra, P.; Li, X.; Bouwman, K. M.; Tompkins, S. M.; Wolfert, M. A.; De Vries, R. P.; Boons, G. J. Heparan Sulfate Proteoglycans as Attachment Factor for SARS-CoV-2. *ACS Cent Sci* **2021**, *7* (6), 1009–1018. https://doi.org/10.1021/ACSCENTSCI.1C00010.

(19) Gstöttner, C.; Zhang, T.; Resemann, A.; Ruben, S.; Pengelley, S.; Suckau, D.; Welsink, T.; Wuhrer, M.; Domínguez-Vega, E. Structural and Functional Characterization of SARS-CoV-2 RBD Domains Produced in Mammalian Cells. *Anal Chem* **2021**, *93* (17), 6839–6847. https://doi.org/10.1021/ACS.ANALCHEM.1C00893.

(20) Tavassoly, O.; Safavi, F.; Tavassoly, I. Heparin-Binding Peptides as Novel Therapies to Stop SARS-CoV-2 Cellular Entry and Infection. *Mol Pharmacol* **2020**, *98* (5), 612. https://doi.org/10.1124/MOLPHARM.120.000098.

(21) Paiardi, G.; Richter, S.; Oreste, P.; Urbinati, C.; Rusnati, M.; Wade, R. C. The Binding of Heparin to Spike Glycoprotein Inhibits SARS-CoV-2 Infection by Three Mechanisms. *J Biol Chem* **2021**, *298* (2), 101507. https://doi.org/10.1016/J.JBC.2021.101507.

(22) Heegaard, N. H. H.; Nilsson, S.; Guzman, N. A. Affinity Capillary Electrophoresis: Important Application Areas and Some Recent Developments. *J Chromatogr B Biomed Appl* **1998**, *715* (1), 29–54. https://doi.org/10.1016/S0378-4347(98)00258-8.

(23) Chen, Z.; Weber, S. G. Determination of Binding Constants by Affinity Capillary Electrophoresis, Electrospray Ionization Mass Spectrometry and Phase-Distribution Methods. *Trends Analyt Chem* **2008**, *27* (9), 738. https://doi.org/10.1016/J.TRAC.2008.06.008.

(24) Sharmeen, S.; Kyei, I.; Hatch, A.; Hage, D. S. Analysis of Drug Interactions with Serum Proteins and Related Binding Agents by Affinity Capillary Electrophoresis: A Review. *Electrophoresis* **2022**, *43* (23–24), 2302–2323. https://doi.org/10.1002/ELPS.202200191;SUBPAGE:STRING:FULL.

(25) Schou, C.; Heegaard, N. H. H. Recent Applications of Affinity Interactions in Capillary Electrophoresis. *Electrophoresis* **2006**, *27* (1), 44–59. https://doi.org/10.1002/ELPS.200500516.

(26) Vergnon, A. L.; Chu, Y. H. Electrophoretic Methods for Studying Protein-Protein Interactions. *Methods: A Companion to Methods in Enzymology* **1999**, *19* (2), 270–277. https://doi.org/10.1006/meth.1999.0856.

(27) Domínguez-Vega, E.; Haselberg, R.; Somsen, G. W.; De Jong, G. J. Simultaneous Assessment of Protein Heterogeneity and Affinity by Capillary Electrophoresis–Mass Spectrometry. *Anal Chem* **2015**, *87* (17), 8781–8788. https://doi.org/10.1021/ACS.ANALCHEM.5B01701.

(28) McKeon, J.; Holland, L. A. Determination of Dissociation Constants for a Heparin-Binding Domain of Amyloid Precursor Protein and Heparins or Heparan Sulfate by Affinity Capillary Electrophoresis. *Electrophoresis* **2004**, *25* (9), 1243–1248. https://doi.org/10.1002/ELPS.200405878.

(29) Chu, Y. H.; Avila, L. Z.; Gao, J.; Whitesides, G. M. Affinity Capillary Electrophoresis. *Acc Chem Res* **2002**, *28* (11), 461–468. https://doi.org/10.1021/AR00059A004.

(30) Chu, Y. H.; Avila, L. Z.; Biebuyck, H. A.; Whitesides, G. M. Use of Affinity Capillary Electrophoresis to Measure Binding Constants of Ligands to Proteins. *J Med Chem* **2002**, *35* (15), 2915–2917. https://doi.org/10.1021/JM00093A027.

(31) Foulds, G. J.; Etzkorn, F. A. A Capillary Electrophoresis Mobility Shift Assay for Protein—DNA Binding Affinities Free in Solution. *Nucleic Acids Res* **1998**, *26* (18), 4304–4305. https://doi.org/10.1093/NAR/26.18.4304.

(32) Heegaard, N. H. H.; Kennedy, R. T. Identification, Quantitation, and Characterization of Biomolecules by Capillary Electrophoretic Analysis of Binding Interactions. https://doi.org/10.1002/(SICI)1522-2683(19991001)20:15/16.

(33) Varenne, A.; Gareil, P.; Colliec-Jouault, S.; Daniel, R. Capillary Electrophoresis Determination of the Binding Affinity of Bioactive Sulfated Polysaccharides to Proteins: Study of the Binding Properties of Fucoidan to Antithrombin. *Anal Biochem* **2003**, *315* (2), 152–159. https://doi.org/10.1016/S0003-2697(02)00687-5.

(34) Huang, Y.; Yang, C.; Xu, X. feng; Xu, W.; Liu, S. wen. Structural and Functional Properties of SARS-CoV-2 Spike Protein: Potential Antivirus Drug Development for COVID-19. *Acta Pharmacol Sin* **2020**, *41* (9), 1141–1149. https://doi.org/10.1038/S41401-020-0485-4;KWRD.

(35) Elshamy, Y. S.; Strein, T. G.; Holland, L. A.; Li, C.; Debastiani, A.; Valentine, S. J.; Li, P.; Lucas, J. A.; Shaffer, T. A. Nanoflow Sheath Voltage-Free Interfacing of Capillary Electrophoresis and Mass Spectrometry for the Detection of Small Molecules. *Anal Chem* **2022**, *94* (32), 11329–11336. https://doi.org/10.1021/ACS.ANALCHEM.2C02074.

(36) Witzel, M. T.; Veltri, L. M.; Kostelic, M.; Elshamy, Y. S.; Lucas, J. A.; Lai, S.; Du, C.; Wysocki, V. H.; Holland, L. A. Protein Analysis Using Capillary Electrophoresis Coupled to Mass Spectrometry through Vibrating Sharp-Edge Spray Ionization. *Electrophoresis* **2024**, *45* (17–18), 1597–1605. https://doi.org/10.1002/ELPS.202300298.

(37) Li, X.; Attanayake, K.; Valentine, S. J.; Li, P. Vibrating Sharp-Edge Spray Ionization (VSSI) for Voltage-Free Direct Analysis of Samples Using Mass Spectrometry. *Rapid Communications in Mass Spectrometry* **2021**, *35* (S1), e8232. https://doi.org/10.1002/RCM.8232.

(38) Ranganathan, N.; Li, C.; Suder, T.; Karanji, A. K.; Li, X.; He, Z.; Valentine, S. J.; Li, P. Capillary Vibrating Sharp-Edge Spray Ionization (CVSSI) for Voltage-Free Liquid Chromatography-Mass Spectrometry. *J Am Soc Mass Spectrom* **2019**, *30* (5), 824–831. https://doi.org/10.1007/S13361-019-02147-0.

(39) Mahmud, S.; Dewasurendra, V. K.; Banerjee, C.; Tavadze, P.; Sultana, M. N.; Rahman, M. A.; Ahmed, S.; Li, P.; Johnson, M. B.; Valentine, S. J. Optimization of Capillary Vibrating Sharp-Edge Spray Ionization for Native Mass Spectrometry of Triplex DNA. *ACS Omega* **2025**, *10* (13), 13131–13140. https://doi.org/10.1021/ACSOMEGA.4C10615.

(40) Greig, M. J.; Gaus, H.; Cummins, L. L.; Sasmor, H.; Griffey, R. H. Measurement of Macromolecular Binding Using Electrospray Mass Spectrometry. Determination of Dissociation Constants for Oligonucleotide: Serum Albumin Complexes. *J*

Am Chem Soc **2002**, *117* (43), 10765–10766. https://doi.org/10.1021/JA00148A028.

(41) Mironov, G. G.; Logie, J.; Okhonin, V.; Renaud, J. B.; Mayer, P. M.; Berezovski, M. V. Comparative Study of Three Methods for Affinity Measurements: Capillary Electrophoresis Coupled with UV Detection and Mass Spectrometry, and Direct Infusion Mass Spectrometry. *J Am Soc Mass Spectrom* **2012**, *23* (7), 1232–1240. https://doi.org/10.1007/S13361-012-0386-Y.

(42) Sharif, D.; Dewasurendra, V. K.; Sultana, M. N.; Mahmud, S.; Banerjee, C.; Rahman, M.; Li, P.; Clemmer, D. E.; Johnson, M. B.; Valentine, S. J. Accessing Different Protein Conformer Ensembles with Tunable Capillary Vibrating Sharp-Edge Spray Ionization. *J Phys Chem B* **2025**, *129* (5), 1626–1639. https://doi.org/10.1021/ACS.JPCB.4C04842.

(43) Chu, Y. H.; Cheng, C. C. Affinity Capillary Electrophoresis in Biomolecular Recognition. *Cellular and Molecular Life Sciences* **1998**, *54* (7), 663–683. https://doi.org/10.1007/S000180050194/METRICS.

(44) Williams, B. A.; Vigh, G. Fast, Accurate Mobility Determination Method for Capillary Electrophoresis. *Anal Chem* **1996**, *68* (7), 1174–1180. https://doi.org/10.1021/AC950968R.

(45) Davis, T. A.; Patberg, S. M.; Sargent, L. M.; Stefaniak, A. B.; Holland, L. A. Capillary Electrophoresis Analysis of Affinity to Assess Carboxylation of Multi-Walled Carbon Nanotubes. *Anal Chim Acta* **2018**, *1027*, 149–157. https://doi.org/10.1016/J.ACA.2018.03.034.

(46) Bowser, M. T.; Chen, D. D. Y. Monte Carlo Simulation of Error Propagation in the Determination of Binding Constants from Rectangular Hyperbolae. 1. Ligand Concentration Range and Binding Constant. *Journal of Physical Chemistry A* **1998**, *102* (41), 8063–8071. https://doi.org/10.1021/JP9819947.